Published in final edited form as:
Cell Rep. 2014 May 22; 7(4): 1184–1196. doi:10.1016/j.celrep.2014.04.003.

Growth of the developing cerebral cortex is controlled by microRNA miR-7 through modifying the p53 pathway

Andrew Pollock[1], **Shan Bian**[1], **Chao Zhang**[3], **Zhengming Chen**[4], and **Tao Sun**[1,2,*]

[1]Department of Cell and Developmental Biology, Weill Medical College of Cornell University, 1300 York Avenue, Box 60, New York, NY 10065, USA

[2]School of Life Sciences and Biotechnology, Shanghai Jiao Tong University, Shanghai 200240, China

[3]Department of Medicine and Institute for Computational Biomedicine

[4]Division of Biostatistics and Epidemiology, Department of Public Health, Weill Medical College of Cornell University, New York, NY 10065, USA

Summary

Proper growth of the mammalian cerebral cortex is crucial for normal brain functions and is controlled by precise gene expression regulation. We here have identified miRNA miR-7 that is highly expressed in cortical neural progenitors, and generated miR-7 sponge transgenic mice in which miR-7 silencing activity is specifically knocked down in the embryonic cortex. Blocking miR-7 function causes microcephaly-like brain defects due to reduced intermediate progenitor (IP) production and apoptosis. Upregulation of miR-7 target genes, including those implicated in the p53 pathway such as Ak1 and Cdkn1a (p21), are responsible for abnormalities in neural progenitors. Furthermore, ectopic expression of Ak1 or p21, and specific blockade of miR-7 binding sites in target genes using protectors *in vivo* are able to recreate reduced IP production. Using conditional miRNA sponge transgenic approaches, we have uncovered an unexpected role for miR-7 in cortical growth through its interactions with genes in the p53 pathway.

Keywords

miR-7; miRNA sponge; p53 pathway; cerebral cortex; intermediate progenitor

*Corresponding author: tas2009@med.cornell.edu, Tel. 212-746-6671; Fax: 212-746-8175.

Author Contributions: AP and TS designed experiments. AP generated all constructs, performed RT-PCR analysis, Northern blotting, *in situ* hybridizations, all luciferase experiments, analyzed mouse model phenotypes, performed tissue collection and preparation, immunostainings, cell counting of immunostainings, TUNEL staining, sequencing tissue collection, and sequencing data analysis. SB performed *in utero* electroporations. CZ and ZC performed DAVID and KEGG analyses. The manuscript was written by AP and TS. TS supervised the project.

Introduction

Formation of the mammalian cerebral cortex requires precise regulation of neural progenitor proliferation and differentiation to generate the proper number of postmitotic neurons. Radial glial cells (RGCs) in the ventricular zone (VZ) are tightly regulated to maintain their own population while producing intermediate progenitors (IPs) that migrate to the subventricular zone (SVZ), and subsequently mature neurons that form the cortical plate (CP) (Götz and Huttner, 2005; Kriegstein et al., 2006; Molyneaux et al., 2007). The proper control of proliferation, survival and differentiation of neural progenitors is crucial for the formation of normal cortical architecture (Rakic, 2009). Expression patterns and levels of genes that govern these processes are modified closely by the molecular mechanisms that are not well understood.

It has recently been demonstrated that microRNAs (miRNAs) are critical for proper neural progenitor development during corticogenesis (Bian and Sun, 2011; De Pietri Tonelli et al., 2008; Kawase-Koga et al., 2010; Nowakowski et al., 2011; Shi et al., 2010). miRNAs are ∼22 nucleotide, endogenous RNAs that guide the RNA-induced silencing complex (RISC) to target messenger RNAs (mRNAs) (Bartel, 2009). Once targeted, the RISC is able to block translation of, or degrade the mRNA transcript (Krol et al., 2010). This posttranscriptional level of regulation is able to fine-tune the expression of target genes and prevent their inappropriate overexpression (Hobert, 2008; Otaegi et al., 2011). Many miRNAs are members of families, or are expressed from multiple loci, giving rise to mature miRNAs with identical seed sequences, making *in vivo* analysis such as gene knockout approach challenging. Promisingly, a miRNA sponge contains complementary binding sequences for the mature miRNAs, titrating them away from their endogenous targets, and in turn knocking down a specific mature miRNA or miRNA family (Ebert et al., 2007; Gentner et al., 2008). Thus, a miRNA sponge provides an effective way to examine the roles of multi-locus miRNAs using a loss-of-function approach.

We here have generated a conditional *miR-7 sponge* transgenic mouse model, in which miR-7 function is specifically knocked down in the cortex. Blocking miR-7 function transiently affects RGC proliferation, however, causes severe defects in progenitor transition from RGCs to IPs, and survival of progenitors, resulting in reduced neurogenesis and dramatically smaller cortex. Illumina RNA sequencing reveals upregulation of 162 of miR-7's predicted target genes in the *miR-7 sponge* cortex, many of which are in the p53 pathway and control cell differentiation and survival. Our results using *miR-7 sponge* transgenic mice have demonstrated a crucial role for miR-7, partly through modifying the p53 pathway, to control neural progenitor specification and survival, and determine cortical size.

Results

miR-7 is expressed in neural progenitors in the VZ/SVZ

Our initial microarray screen for miRNAs expressed in mouse developing cortices revealed miR-7 expression at embryonic day 12.5 (E12.5) and postnatal day 0 (P0). Mature miR-7 with highly conserved seed sequences is processed from three precursors—miR-7a-1,

miR-7a-2 and miR-7b, which are transcribed from separate loci on chromosomes 13, 7 and 17, respectively, in mice (Figure 1A). To verify expression levels of miR-7 in embryonic cortices, we performed Northern blot analyses and detected mature miR-7 in cortices of E12.5 and throughout development, using a locked nucleic acid (LNA) probe for miR-7a, which can also detect miR-7b (Figure 1B). Next we used quantitative real-time reverse transcription PCR (qRT-PCR) to determine which loci were most highly expressed in developing cortices. While miR-7a-2 and 7b showed low levels of expression, miR-7a-1 was the primary source of miR-7, with expression levels more than 25 times that of miR-7a-2 and close to 12 times that of miR-7b in the E15.5 cortex (Figure 1C). To further examine the expression pattern of miR-7 in developing cortices, we used the miR-7a LNA probe for *in situ* hybridization. miR-7a was expressed in the VZ and SVZ in E12.5 cortices and was maintained there through P0 (Figures 1D-1G). miR-7 expression was also detected in the subplate and the cortical plate in E15.5 and P0 cortices (Figures 1F and 1G). These findings suggest that miR-7 may play an important role in neural progenitor development throughout cortical development.

miR-7 sponge blocks the silencing effect of miR-7 on target genes *in vitro*

To test the role of miR-7 in cortical development using a loss-of-function approach, we designed a bulged miR-7 sponge to simultaneously block the silencing activity of miR-7 transcribed from all three separate loci (Figure 1H). The miR-7 sponge (7-sp) consisted of 24 narrowly spaced, bulged binding sites for miR-7 (Otaegi et al., 2012). Mature miR-7a and miR-7b sequences differ by only a single base, and this was designed to fall within the bulge region of the sponge, so the sponge should affect the function of all three precursors equally by titrating mature miR-7 away from its endogenous targets, and leaving them unbound by miR-7 (Figure S1A). We also designed a scrambled sponge construct (Scr-sp) whose architecture is the same, except that the binding site sequence is predicted to be untargeted by any miRNA (Figure 1I) (Gentner et al., 2008).

To test the function of these sponges, we designed a luciferase assay, attaching a 3′UTR containing the miR-7 targeting site to the *luciferase* gene. All three precursors of miR-7, but not control miRNA miR-17 or a miR-7 construct with a mutated seed sequence, caused a reduction in luciferase activity (Figure 1J and Figure S1B). miR-7 sponge was then attached to the 3′UTR of a gene encoding *iCre* and co-expressed with the three different miR-7 precursors, and the *luciferase* gene with a miR-7 targeting site in its 3′UTR. Reduced luciferase activity due to any of the three miR-7 precursors was significantly rescued by the miR-7 sponge but not by a scrambled sponge (Figure 1J). Additionally, a miR-7 sponge with 3 mutations in the binding seed sequence was unable to rescue reductions caused by miR-7 (Figure S1B). Our results demonstrate that the miR-7 sponge is able to block the function of miR-7 transcribed from any of the three loci.

miR-7 sponge transgenic mice present smaller cortex

To examine the function of miR-7 in cortical development *in vivo*, we generated conditional *miR-7 sponge* transgenic mice. To make the transgene construct, the constitutively active *CAG* promoter was used to drive expression of a floxed transcriptional stop signal, followed by a coding gene—destabilized *green fluorescent protein* D2e*GFP* with the 24-bulged

miR-7 sponge sites inserted as its 3′UTR (Figure 2A). Transgene injection generated two transgenic founder lines (line 12 and 17), called *miR-7 sponge* (*7-sp*) carrier mice, which showed no distinguishable phenotypes. To activate miR-7 sponge activity in the cortex, *miR-7 sponge* carrier mice were bred with an *Emx1-Cre* line expressing *Cre* in the embryonic dorsal cortical region beginning by E10.5 (Gorski et al., 2002). *Emx1-Cre:miR-7 sponge* transgenic mice, called *7-sp* mice, showed detectably smaller cortices even at E12.5, with dramatically reduced cortical size at E15.5 and P0 with 100% penetrance (Figure 2B). Lines 12 and 17 showed indistinguishable phenotypes, so all analysis shown here is of line 17.

We used the same system to generate a conditional transgenic scrambled sponge mouse. Transgene injection generated 5 founder lines and again, carrying the transgene alone had no phenotype. Unlike *7-sp* mice, however, activation of the scrambled sponge using the *Emx1-Cre* line, called *Scr-sp* mice, caused no discernible changes in the cortex in any founder line at all tested stages, so all analysis shown here is of line 38 (Figure 2B). Our results indicate that blocking miR-7 silencing activity in the cortex causes microcephaly-like brain defects.

miR-7-sponge blocks miR-7 function *in vivo* without affecting other miRNAs

To demonstrate the specific activation of miR-7 sponge transgene, we expressed a non-fluorescent *pCAG-iCre* plasmid and a sensor construct for miR-7 in cortices of E13.5 *7-sp* carrier mice using *in utero* electroporation. Wild-type littermates received the same electroporation to serve as a control. The sensor plasmid contained the *enhanced GFP* (*eGFP*) and *monomeric RFP* (*mRFP*) reporter genes, each transcribed from a separate promoter. *eGFP* had no 3′UTR while *mRFP* contained 2 binding sites for miR-7 in its 3′UTR (Figure 2C). Therefore, in electroporated wild-type cortices, all cells that receive the plasmid should express eGFP, while mRFP that is sensitive to miR-7 silencing, will be expressed only in cells where it cannot sense miR-7. In electroporated *7-sp* carrier cortices, in cells co-electroporated with *iCre*, miR-7 should be blocked by the miR-7 sponge transgene, allowing mRFP expression. Meanwhile a subset of cells may not receive *iCre* co-electroporation. These will still have functioning miR-7, and thus express no mRFP (Figure 2C).

48 hours after electroporation, only ∼10% of electroporated cells were found to express mRFP in the VZ/SVZ of the control cortex, confirming that most neural progenitors express endogenous miR-7, although interestingly, a sub-population of cells in the VZ/SVZ do not. On the other hand, in *7-sp* carrier cortices, over 30% of electroporated cells expressed mRFP (Figures 2D and 2E). This increase indicates that in cells that normally express miR-7, expression of the sponge is able to block miR-7 function *in vivo*. And as predicted, a population of cells appeared green, likely due to unsuccessful co-electroporation of the *iCre* plasmid. Conversely, electroporation of a sensor for control miRNA miR-9 revealed strong miR-9 activity in nearly all electroporated cells, with no obvious change when the miR-7 sponge transgene is activated (Figure S2). Our results indicate that once activated, the *miR-7 sponge* transgene is able to specifically block the activity of endogenous miR-7 but not miR-9 in cells in the VZ/SVZ of developing cortices.

miR-7 functional knockdown causes reduced neurogenesis

To examine what may cause reduced cortical size in *miR-7 sponge* mice, we first assessed whether neural production or cortical layer organization was affected. We examined the expression of Tbr1 (layer 6), Ctip2 (Layer 5) and Cux1 (Layer 2/3) in P0 *7-sp* and control cortices (Molyneaux et al., 2007). The relative positioning of layer markers in the CP was similar to wild-type, suggesting that overall cortical layer organization was not greatly affected by miR-7 blockade (Figure 3). However, each layer examined was thinner, with significantly fewer mature $NeuN^+$ neurons found, and significant reductions in the number of early-born $Tbr1^+$ and $Ctip2^+$ neurons, and late-born $Cux1^+$ neurons (Figure 3). On the other hand, scrambled sponge activation caused no detectable defects compared to controls using any of the assessed markers, suggesting that ectopic expression of a sponge transcript without miRNA binding sites has no effects on cortical neurogenesis (Figure S3). Moreover, TUNEL staining showed no increase in dying cells in P0 *7-sp* cortices, suggesting that cell survival is not affected by the miR-7 sponge at postnatal stages. Our results indicate that miR-7 is required for proper neurogenesis but not overall organization of both early- and late-born neuronal subtypes in different cortical layers.

RGCs are transiently affected by reduced miR-7 activity

To understand the causes of reduced neurogenesis in the *miR-7 sponge* cortex, we examined neural progenitor development. *Emx1-Cre* is activated by E10.5, so we should be able to detect changes in the number of neural progenitors at E12.5. The number of actively cycling progenitors, measured by Ki67 expression, was slightly reduced, and so was BrdU incorporation in the E12.5 *7-sp* cortex compared to controls (Figures 4A-4C). The cell cycle labeling index (LI), however, was similar to controls (Figure 4D). The number of $PH3^+$ cells in the M-phase of the cell cycle was also not changed (Figures 4E and 4F). Correspondingly we detected a slight reduction in the number of $Pax6^+$ RGCs, however, the number of cycling RGCs which took up BrdU was similar to controls, suggesting that the mild defect in RGC numbers was not related to their ability to proliferate (Figures 4G and 4H). By later stages, the progenitor pool recovered from its mild defects. The overall numbers of $Ki67^+$ progenitors, and $Pax6^+$ RGCs were restored to control levels in E15.5 *7-sp* cortices, and cell cycle parameters remained similar to controls (Figures 4I-4P). The numbers and the cell cycle LI of neural progenitors in *Scr-sp* cortices were similar to those in controls at both E12.5 and E15.5 (Figure S4). Our results indicate that blocking the activity of miR-7 has only mild, transient effects on RGCs in the embryonic cortex.

miR-7 function is required for intermediate progenitor transition and survival

Since the number of RGCs was largely unaffected but neurogenesis was significantly reduced in embryonic *miR-7-sp* cortices, we assessed whether loss of miR-7 function affects IPs by examining the expression of the IP marker Tbr2. Unlike RGCs, the number of $Tbr2^+$ cells remained significantly reduced in *7-sp* cortices from E12.5 through E15.5 (Figures 5A-5K). However, in *Scr-sp* cortices the number of Tbr2 expressing IPs was not affected (Figure S5). In *7-sp* cortices, the number of cells that co-express Pax6 and Tbr2, labeling IPs under transition from RGCs, was halved at both E12.5 and E15.5, indicating that miR-7 function is required for normal IP transition (Figures 5C and 5F). At both E12.5 and E15.5,

the number of $Tbr2^+/BrdU^+$ cells was also reduced in company with overall $Tbr2^+$ cell reductions, leading to an IP cell cycle labeling index not significantly different from controls (Figures 5G-5L). These results suggest that while the number of IPs was significantly reduced, the behavior of existing IPs remained similar to controls.

We next tested whether survival of neural progenitors was affected by miR-7 blockade using a combination of a TUNEL assay with immunofluorescence for Pax6 or Tbr2. While control or *scrambled sponge* brains showed little cell death, E12.5 *miR-7 sponge* brains displayed large numbers of $TUNEL^+$ cells that were mostly localized in the SVZ (Figures 5M and 5N, and Figure S5C). At E15.5, individual $TUNEL^+$ cells could still be seen in *miR-7 sponge*, but not significantly in *Scr-sp* cortices (Figures 5O and 5P, and Figure S5F). Most $TUNEL^+$ cells were detected in the SVZ and intermediate zone (IZ), but not in the CP (Figures 5O and 5P). These results suggest that miR-7 function is required for neural progenitors, largely in the SVZ, to differentiate and survive.

miR-7 controls neurogenesis through suppressing multiple genes

We next assessed the underlying mechanism of miR-7 regulation in cortical development by identifying its target genes. miRNAs can have many simultaneous targets *in vivo*, so in order to determine which targets may be responsible for the phenotypes in *miR-7 sponge* mice, we used an Illumina RNA sequencing approach (Figure 6A). This approach provides a global view of alterations to the transcriptome due to manipulation of miR-7 with the expectation that miR-7 target genes released from regulation by miR-7 sponge will be upregulated. Total RNA was isolated from E12.5 dorsal cortices of three *7-sp* and three wild-type littermate embryos, sequenced and analyzed using GobyWeb (Dorff et al., 2013). Overall gene expression was not greatly different from wild-type with only a few genes exhibiting large deviations from controls (Figure 6B). On detailed analysis of expressed genes, we found that 419 genes had been consistently upregulated by at least 25%. Gene ontology (GO) analysis was performed using Gorilla (Eden et al., 2007; Eden et al., 2009). Genes related to proliferation, cell death or survival and differentiation were found to be significantly overrepresented among upregulated genes, suggesting a molecular basis for the observed neurogenesis defects in *7-sp* cortices (Figure 6C).

To determine which genes may be direct targets of miR-7, we compared the list of upregulated genes to lists of predicted miRNA targets using 5 target prediction algorithms (miRWalk, Targetscan, Miranda, miRDB and RNA22) via the miRWalk tool. 162 out of the 419 upregulated genes were predicted targets of miR-7. We next generated an expected number of genes that a non-specific miRNA would target in our set of 419 upregulated genes by comparing the 419 genes to target lists for 35 other miRNAs, including the 20 highest expressed neural miRNAs and additional known neural miRNAs (Chi et al., 2009). We found that the mean expected number of predicted targets by these baseline miRNAs is approximately 111 +/- 4.2 SEM, similar to the number of predicted targets for a heart specific miRNA miR-1. However, 162 predicted targets of miR-7 were more than 2 standard deviations above the non-specific expectation (Figure 6D). Taken with our miR-7 sensor assay (Figure 2), these results strongly suggest that the phenotype in *miR-7 sponge* cortices is due to specific blockade of miR-7 function, and upregulation of miR-7 target genes.

miR-7 targets the p53 signaling pathway at multiple points

We hypothesized that rather than targeting individual genes, miR-7 may attempt to regulate whole pathways by silencing multiple genes within that pathway. To test this we performed KEGG pathway analysis on the 162 genes which were both upregulated and predicted miR-7 targets using David 6.7 (Figure 6E and Figure S6) (Huang et al., 2008). This analysis uncovered that 6 out of 162 genes are annotated as being part of the p53 signaling pathway, a highly significant overrepresentation. Agilent Literature Search Software v2.8 and subsequent manual confirmation based on PubMed confirmed these 6 and more showing a total of 19 out of 162 miR-7 target genes fall into the p53 pathway (Figure 6F). According to the GO annotations of these genes, most were involved in regulating cell cycle arrest, cell death and cell differentiation, suggesting underlying causes of *miR-7-sp* cortical defects.

miR-7 directly regulates multiple genes in the p53 pathway in the cortex

To confirm that these predicted genes can be directly targeted by miR-7, we used luciferase assays, attaching the 3′UTR of each gene to a *luciferase* reporter. We selected 5 predicted miR-7 target genes, each associated with the p53 pathway, and with known functions regulating differentiation or survival in neural development: a cytosolic *adenylate kinase Ak1*, apoptotic activator *Pmaip1* (also known as *Noxa*), CDK inhibitor *Cdkn1a* (also known as *p21*), transcription factor *Klf4*, and the cyclin *Ccng1* (Akhtar et al., 2006; Lookeren Campagne and Gill, 1998; Noma et al., 1999; Qin and Zhang, 2012). Furthermore, all of them showed significant upregulation of expression levels *in vivo* due to loss of miR-7 function (Figure S6). When co-expressed with miR-7 *in vitro*, the 3′UTRs of each of these genes were targeted by miR-7a, resulting in significant reduction of luciferase activity (Figure 7A). Luciferase reductions were not induced by co-expression with a control miRNA miR-17 (with the exception of p21, a known target of miR-17) or by a mutated miR-7 (Figure 7A) (Wong et al., 2010). Our results indicate that these 5 genes in the p53 pathway are putative targets for miR-7.

We next assessed whether upregulation of these genes *in vivo* contributes to some of the phenotypes found in *miR-7-sp* cortices. The full length cDNA for *Ak1* or *p21* was ectopically expressed in E13.5 cortices using *in utero* electroporation, and embryos were analyzed after 24 hours. Consistent with the *7-sp* cortical phenotype, ectopic expression of either *Ak1* or *p21* had no effect on the percentage of electroporated cells expressing Pax6 relative to electroporation with an empty pCAGIG vector. However, there was a significant reduction in the relative percentage of Tbr2-expressing cells, suggesting a specific reduction in IP generation (Figures 7B and 7C). Activated Caspase3 expression was not significantly altered due to ectopic expression of *Ak1* or *p21*. These results suggest that suppression of Ak1 and p21 is necessary for successful generation of IP.

Finally, to examine the specific interaction between miR-7 and target genes *in vivo*, we co-electroporated pCAGIG with LNA target protectors—oligos designed to bind specifically to the miR-7 binding site in the 3′UTR of *Ak1* or *p21*, preventing miR-7 from silencing its targets. Additionally, we generated a control protector against an alternate site on the *Ak1* 3′UTR, which should not affect miR-7 binding. Electroporation of the control protector elicited no changes relative to the no-oligo condition. Electroporation of protectors blocking

miR-7's interaction with *Ak1* or *p21*, however, closely mimicked overexpression of these genes, with no changes in the relative percentage of $Pax6^+$ cells, and slight but significant reductions in the percentage of $Tbr2^+$ cells (Figures 7D and 7E). Again, activated Caspase3 expression was not significantly altered. All together, these results demonstrate that miR-7 function is crucial for neural progenitors to successfully produce IPs, and furthermore that this process is partly mediated by the p53 pathway genes Ak1 and p21 in the developing cortex.

Discussion

Because the proper cortical size is essential for brain functions, identifying molecules that control cortical growth will help understand how brain malformations occur. In this work we have generated a mouse model in which the activity of miR-7, processed from all three primary loci, is specifically knocked down in the cortex using a miR-7 sponge. We have shown that *miR-7 sponge* mice have significantly smaller cortices, and that miR-7 activity is required for the RGC to IP transition, and for progenitor survival in the SVZ. miR-7 function is carried out at least partly through direct regulation of the p53 pathway genes such as Ak1 and p21. Our studies have uncovered a crucial role of noncoding RNAs in cortical size control.

Proper growth of the cortex relies on expansion of both RGCs and IPs (Lui et al., 2011; Molnar and Clowry, 2012; Rakic, 2009). Recent studies have shown that specification, proliferation and differentiation of IPs are essential for controlling the neural progenitor pool and cortical growth (Arnold et al., 2008; Englund et al., 2005; Sessa et al., 2010; Sessa et al., 2008). The importance of miRNAs in controlling cortical growth is becoming evident. The miR-17-92 cluster has been shown to control cortical size by regulating RGC proliferation and IP specification (Bian et al., 2013; Nowakowski et al., 2013). Our studies here have shown that blocking miR-7 silencing activity in *miR-7 sponge* transgenic mice has only a mild transient effect on the apical progenitor pool. IP production, however, is severely impaired throughout neurogenesis, suggesting that this act of progenitor specification serves as a checkpoint that is failed by cells lacking miR-7 function. It has been previously shown that IPs are responsible for producing neurons in all layers of the cortical plate (Kowalczyk et al., 2009). The more severe reduction of upper layer neurons than deep layer neurons is likely caused by continuous impairment of expansion of IPs but not RGCs in *miR-7 sponge* cortices. Our studies have demonstrated a new mechanism, regulated by miR-7, which controls the IP population and in turn brain size. Moreover, it is likely miR-7 plays multiple roles in many aspects of brain development. In dissociated cortical neurons, miR-7 has been found to repress neurite outgrowth, promote oligodendrocyte differentiation, and regulate α-synuclein, suggesting a role in Parkinson's Disease (Chen et al., 2010; Doxakis, 2010; Junn et al., 2009; Zhao et al., 2012). More recently, miR-7 has been shown to repress olfactory dopamine neuron development in mice (de Chevigny et al., 2012). These studies indicate that miR-7, working together with protein-coding genes, is a major neuronal miRNA that is essential for brain development and functions.

Uncovering the full scope of a miRNA's function can be challenging. miRNAs can target many genes simultaneously, and it is difficult to isolate any one target from the global

context in a loss-of-function model. Furthermore, these interactions can be distinct in different contexts and cell types. By using Illumina sequencing and pathway analysis, we have identified a wide network of pathways targeted by miR-7. In fact, the total number of altered targets is likely even higher because RNA sequencing will not detect changes in targets whose mRNA is not degraded by miR-7. Organizing miRNA targets into pathways in this way gives an overall picture of the miRNA's functions in a complex process like neuronal differentiation, and provides more avenues for further study than analyzing single targets.

We have found that while other pathways are also revealed to be targeted by miR-7, functions of the p53 pathway are closely associated with the defects in the *7-sp* cortex. The p53 pathway, overlapping with those of its cortically expressed family members p63 and p73, is intimately linked to cell cycle checkpoint control and cell survival (Murray-Zmijewski et al., 2008). Verified miR-7 targets Ak1 and Klf4 have been implicated in neuronal differentiation (Inouye et al., 1998; Noma et al., 1999; Qin and Zhang, 2012). Ccng1 and p21 have been shown to promote cell cycle arrest that can lead to apoptosis (El-Deiry et al., 1993; Wade Harper et al., 1993). Pmaip1 (Noxa) has been described as an executor of p53-mediated apoptosis, although its role may be less pronounced in neurons (Akhtar et al., 2006; Michalak et al., 2008). By blocking miR-7 interactions with specific genes in the p53 pathway, we can partially phenocopy the *7-sp* phenotype. Noticeably, blocking miR-7's interaction with even a single target using a miR-7 target protector recapitulates reduced generation of Tbr2-expressing IPs, although it fails to recreate the cell death defect. Apoptosis in *miR-7 sponge* cortices may well be a result of altered expression of a combination of the 162 upregulated genes, or an indirect outcome of miR-7 manipulation.

Furthermore, the generation of conditional *miR-7 sponge* transgenic mouse model has provided a useful tool to investigate miRNA functions *in vivo*. The sponge of miRNAs can block activities of all miRNA precursors, and avoid the generation of miRNA knockout mice that are expensive and time consuming. The conditional sponge transgenic mice also allow tissue- and cell type-specific investigation of miRNA functions.

Taken together, our results indicate that miR-7 plays a critical role in cortical neurogenesis by modulating the expression levels of multiple targets. Regulation of targets Ak1, p21, and likely others in the p53 pathway permits proper RGC to IP transition, prevents progenitor apoptosis, and allows subsequent neuronal production in order to control normal brain size.

Experimental procedures

Sponge transgene and transgenic mouse generation

We generated the conditional transgenic expression construct, called here *pCBR*, using the *pBigT* vector as a backbone. The constitutively active *CAG* promoter was subcloned from the *pCAGIG* vector into the construct to drive transgene expression. Forward and reverse sponge oligos containing 3 bulged miR-7, miR-7 with 3 mutations in the binding seed, or scrambled binding sites were flanked by the *Spe*I and *Xba*I cutting sites (Table S1). Oligos were annealed and additively cloned to finally contain 24 binding sites. This sponge

sequence was subcloned in the 3′UTR of D2*eGFP* and then into the *pCBR* conditional expression vector.

To verify transgene activation, the miR-7- or scrambled- sponges in the *pCBR* vector were co-transfected with *pCDNA-iCre* expression construct into Neuro2A cells. The sponge D2eGFP was detectable by a Western Blot using anti-GFP antibodies.

The transgene fragment was released by *Kpn*I digestion for generating transgenic mice at the Weill Cornell transgenic core facility. *miR-7-Sp* carrier mice were generated on a C57BL/6J background, *Scrambled sponge* mice were generated on an F1 background. Potential founders were screened by PCR for D2*eGFP* and the *Neo* cassette.

Transgene activation and genotyping

Sponge transgenes were activated in the embryonic dorsal cortical region *in vivo* by crossing transgene carrier mice to the *Emx1-Cre* line (The Jackson Laboratory) to generate *Emx1-Cre:miR-7 sponge* or *Emx1-Cre:Scrambled-Sponge*, called here *7-sp* or *Scr-sp*. For staging of embryos, midday of the day of vaginal-plug formation was considered as E0.5; the first 24 hours after birth were defined as P0. Animal use was overseen by the Animal Facility at the Weill Cornell Medical College. For mouse genotyping, mouse tail-tip or embryonic tail biopsies were used for PCR reactions using primer pairs to detect *Cre*, *Neomycin* or D2*eGFP* (Table S1).

Statistics

For electroporated mouse sections, at least three brains from each group were analyzed. Statistical comparison was made by an analysis of variance (unpaired Student's *t*-Test).

Supplementary Material

Refer to Web version on PubMed Central for supplementary material.

Acknowledgments

We thank Dr. Frank Costantini at Columbia University for providing the *pBigT* plasmid. This work was supported by the Weill Cornell Training Program in Stem Cell Biology and Regenerative Medicine (NYSTEM), New York State Department of Health, C026878 (A. P.), the Clinical Translational Science Center, National Center for Advancing Translational Sciences (UL1-RR024996) (Z. C.), the Hirschl/Weill-Caulier Trust (T. S.), an NPRP grant (09-1011-3-260) from the Qatar National Research Fund and an R01-MH083680 grant from the NIH/NIMH (T. S.).

References

Akhtar RS, Geng Y, Klocke BJ, Latham CB, Villunger A, Michalak EM, Strasser A, Carroll SL, Roth KA. BH3-Only Proapoptotic Bcl-2 Family Members Noxa and Puma Mediate Neural Precursor Cell Death. The Journal of Neuroscience. 2006; 26:7257–7264. [PubMed: 16822983]

Arnold SJ, Huang GJ, Cheung AF, Era T, Nishikawa S, Bikoff EK, Molnar Z, Robertson EJ, Groszer M. The T-box transcription factor Eomes/Tbr2 regulates neurogenesis in the cortical subventricular zone. Genes Dev. 2008; 22:2479–2484. [PubMed: 18794345]

Bartel DP. MicroRNAs: Target Recognition and Regulatory Functions. Cell. 2009; 136:215–233. [PubMed: 19167326]

Bian S, Hong J, Li Q, Schebelle L, Pollock A, Knauss Jennifer L, Garg V, Sun T. MicroRNA Cluster miR-17-92 Regulates Neural Stem Cell Expansion and Transition to Intermediate Progenitors in the Developing Mouse Neocortex. Cell Reports. 2013; 3:1398–1406. [PubMed: 23623502]

Bian S, Sun T. Functions of Noncoding RNAs in Neural Development and Neurological Diseases. Molecular Neurobiology. 2011; 44:359–373. [PubMed: 21969146]

Chen H, Shalom-Feuerstein R, Riley J, Zhang SD, Tucci P, Agostini M, Aberdam D, Knight RA, Genchi G, Nicotera P. miR-7 and miR-214 are specifically expressed during neuroblastoma differentiation, cortical development and embryonic stem cells differentiation, and control neurite outgrowth in vitro. Biochemical and Biophysical Research Communications. 2010; 394:921–927. [PubMed: 20230785]

Chi SW, Zang JB, Mele A, Darnell RB. Argonaute HITS-CLIP decodes microRNA–mRNA interaction maps. Nature. 2009

de Chevigny A, Core N, Follert P, Gaudin M, Barbry P, Beclin C, Cremer H. miR-7a regulation of Pax6 controls spatial origin of forebrain dopaminergic neurons. Nat Neurosci. 2012; 15:1120–1126. [PubMed: 22729175]

De Pietri Tonelli D, Pulvers JN, Haffner C, Murchison EP, Hannon GJ, Huttner WB. miRNAs are essential for survival and differentiation of newborn neurons but not for expansion of neural progenitors during early neurogenesis in the mouse embryonic neocortex. Development. 2008; 135:3911–3921. [PubMed: 18997113]

Dorff KC, Chambwe N, Zeno Z, Simi M, Shaknovich R, Campagne F. GobyWeb: Simplified Management and Analysis of Gene Expression and DNA Methylation Sequencing Data. PLoS ONE. 2013; 8:e69666. [PubMed: 23936070]

Doxakis E. Post-transcriptional Regulation of α-Synuclein Expression by mir-7 and mir-153. Journal of Biological Chemistry. 2010; 285:12726–12734. [PubMed: 20106983]

Ebert MS, Neilson JR, Sharp PA. MicroRNA sponges: competitive inhibitors of small RNAs in mammalian cells. Nature Methods. 2007; 4:721–726. [PubMed: 17694064]

Eden E, Lipson D, Yogev S, Yakhini Z. Discovering Motifs in Ranked Lists of DNA Sequences. PLoS Comput Biol. 2007; 3:e39. [PubMed: 17381235]

Eden E, Navon R, Steinfeld I, Lipson D, Yakhini Z. GOrilla: a tool for discovery and visualization of enriched GO terms in ranked gene lists. BMC Bioinformatics. 2009; 10:48. [PubMed: 19192299]

El-Deiry WS, Tokino T, Velculescu VE, Levy DB, Parsons R, Trent JM, Lin D, Mercer WE, Kinzler KW, Vogelstein B. WAF1, a potential mediator of p53 tumor suppression. Cell. 1993; 75:817–825. [PubMed: 8242752]

Englund C, Fink A, Lau C, Pham D, Daza RA, Bulfone A, Kowalczyk T, Hevner RF. Pax6, Tbr2, and Tbr1 are expressed sequentially by radial glia, intermediate progenitor cells, and postmitotic neurons in developing neocortex. J Neurosci. 2005; 25:247–251. [PubMed: 15634788]

Gentner B, Schira G, Giustacchini A, Amendola M, Brown BD, Ponzoni M, Naldini L. Stable knockdown of microRNA in vivo by lentiviral vectors. Nature Methods. 2008; 6:63–66. [PubMed: 19043411]

Gorski JA, Talley T, Qiu M, Puelles L, Rubenstein JLR, Jones KR. Cortical Excitatory Neurons and Glia, But Not GABAergic Neurons, Are Produced in the Emx1-Expressing Lineage. The Journal of Neuroscience. 2002; 22:6309–6314. [PubMed: 12151506]

Götz M, Huttner WB. The cell biology of neurogenesis. Nat Rev Mol Cell Biol. 2005; 6:777–788. [PubMed: 16314867]

Hobert O. Gene Regulation by Transcription Factors and MicroRNAs. Science. 2008; 319:1785–1786. [PubMed: 18369135]

Huang DW, Sherman BT, Lempicki RA. Systematic and integrative analysis of large gene lists using DAVID bioinformatics resources. Nat Protocols. 2008; 4:44–57.

Inouye S, Seo M, Yamada Y, Nakazawa A. Increase of Adenylate Kinase Isozyme 1 Protein During Neuronal Differentiation in Mouse Embryonal Carcinoma P19 Cells and in Rat Brain Primary Cultured Cells. Journal of Neurochemistry. 1998; 71:125–133. [PubMed: 9648858]

Junn E, Lee KW, Jeong BS, Chan TW, Im JY, Mouradian MM. Repression of -synuclein expression and toxicity by microRNA-7. Proceedings of the National Academy of Sciences. 2009; 106:13052–13057.

Kawase-Koga Y, Low R, Otaegi G, Pollock A, Deng H, Eisenhaber F, Maurer-Stroh S, Sun T. RNAase-III enzyme Dicer maintains signaling pathways for differentiation and survival in mouse cortical neural stem cells. Journal of Cell Science. 2010; 123:586–594. [PubMed: 20103535]

Kowalczyk T, Pontious A, Englund C, Daza RAM, Bedogni F, Hodge R, Attardo A, Bell C, Huttner WB, Hevner RF. Intermediate Neuronal Progenitors (Basal Progenitors) Produce Pyramidal–Projection Neurons for All Layers of Cerebral Cortex. Cerebral Cortex. 2009; 19:2439–2450. [PubMed: 19168665]

Kriegstein A, Noctor S, Martinez-Cerdeno V. Patterns of neural stem and progenitor cell division may underlie evolutionary cortical expansion. Nat Rev Neurosci. 2006; 7:883–890. [PubMed: 17033683]

Krol J, Loedige I, Filipowicz W. The widespread regulation of microRNA biogenesis, function and decay. Nat Rev Genet. 2010; 11:597–610. [PubMed: 20661255]

Lookeren Campagne MV, Gill R. Tumor-suppressor p53 is expressed in proliferating and newly formed neurons of the embryonic and postnatal rat brain: Comparison with expression of the cell cycle regulators p21Waf1/Cip1, p27Kip1, p57Kip2, p16Ink4a, cyclin G1, and the proto-oncogene bax. The Journal of Comparative Neurology. 1998; 397:181–198. [PubMed: 9658283]

Lui JH, Hansen DV, Kriegstein AR. Development and evolution of the human neocortex. Cell. 2011; 146:18–36. [PubMed: 21729779]

Michalak EM, Villunger A, Adams JM, Strasser A. In several cell types tumour suppressor p53 induces apoptosis largely via Puma but Noxa can contribute. Cell Death Differ. 2008; 15:1019–1029. [PubMed: 18259198]

Molnar Z, Clowry G. Cerebral cortical development in rodents and primates. Prog Brain Res. 2012; 195:45–70. [PubMed: 22230622]

Molyneaux BJ, Arlotta P, Menezes JR, Macklis JD. Neuronal subtype specification in the cerebral cortex. Nat Rev Neurosci. 2007; 8:427–437. [PubMed: 17514196]

Murray-Zmijewski F, Slee EA, Lu X. A complex barcode underlies the heterogeneous response of p53 to stress. Nat Rev Mol Cell Biol. 2008; 9:702–712. [PubMed: 18719709]

Noma T, Yoon YS, Nakazawa A. Overexpression of NeuroD in PC12 cells alters morphology and enhances expression of the adenylate kinase isozyme 1 gene. Molecular Brain Research. 1999; 67:53–63. [PubMed: 10101232]

Nowakowski TJ, Fotaki V, Pollock A, Sun T, Pratt T, Price DJ. MicroRNA-92b regulates the development of intermediate cortical progenitors in embryonic mouse brain. Proceedings of the National Academy of Sciences. 2013; 110:7056–7061.

Nowakowski TJ, Mysiak KS, Pratt T, Price DJ. Functional dicer is necessary for appropriate specification of radial glia during early development of mouse telencephalon. PLoS One. 2011; 6:e23013. [PubMed: 21826226]

Otaegi G, Pollock A, Hong J, Sun T. MicroRNA miR-9 Modifies Motor Neuron Columns by a Tuning Regulation of FoxP1 Levels in Developing Spinal Cords. Journal of Neuroscience. 2011; 31:809–818. [PubMed: 21248104]

Otaegi G, Pollock A, Sun T. An optimized sponge for microRNA miR-9 affects spinal motor neuron development in vivo. Frontiers in Neuroscience. 2012; 5

Qin S, Zhang CL. Role of Krüppel-Like Factor 4 in Neurogenesis and Radial Neuronal Migration in the Developing Cerebral Cortex. Molecular and Cellular Biology. 2012; 32:4297–4305. [PubMed: 22907754]

Rakic P. Evolution of the neocortex: a perspective from developmental biology. Nat Rev Neurosci. 2009; 10:724–735. [PubMed: 19763105]

Sessa A, Mao CA, Colasante G, Nini A, Klein WH, Broccoli V. Tbr2-positive intermediate (basal) neuronal progenitors safeguard cerebral cortex expansion by controlling amplification of pallial glutamatergic neurons and attraction of subpallial GABAergic interneurons. Genes Dev. 2010; 24:1816–1826. [PubMed: 20713522]

Sessa A, Mao CA, Hadjantonakis AK, Klein WH, Broccoli V. Tbr2 directs conversion of radial glia into basal precursors and guides neuronal amplification by indirect neurogenesis in the developing neocortex. Neuron. 2008; 60:56–69. [PubMed: 18940588]

Shi Y, Zhao X, Hsieh J, Wichterle H, Impey S, Banerjee S, Neveu P, Kosik KS. MicroRNA Regulation of Neural Stem Cells and Neurogenesis. The Journal of Neuroscience. 2010; 30:14931–14936. [PubMed: 21068294]

Wade Harper J, Adami GR, Wei N, Keyomarsi K, Elledge SJ. The p21 Cdk-interacting protein Cip1 is a potent inhibitor of G1 cyclin-dependent kinases. Cell. 1993; 75:805–816. [PubMed: 8242751]

Wong P, Iwasaki M, Somervaille TCP, Ficara F, Carico C, Arnold C, Chen CZ, Cleary ML. The miR-17-92 microRNA Polycistron Regulates MLL Leukemia Stem Cell Potential by Modulating p21 Expression. Cancer Research. 2010; 70:3833–3842. [PubMed: 20406979]

Zhao X, Wu J, Zheng M, Gao F, Ju G. Specification and maintenance of oligodendrocyte precursor cells from neural progenitor cells: involvement of microRNA-7a. Molecular Biology of the Cell. 2012; 23:2867–2877. [PubMed: 22696677]

Highlights

- The miR-7 sponge is sufficient to block silencing activity of three miR-7 precursors.
- Cortical specific miR-7 sponge transgenic mice show microcephaly-like brain defects.
- Expansion and survival of cortical intermediate progenitors require miR-7 function.
- miR-7 modifies expression levels of genes in the p53 pathway in the embryonic cortex.

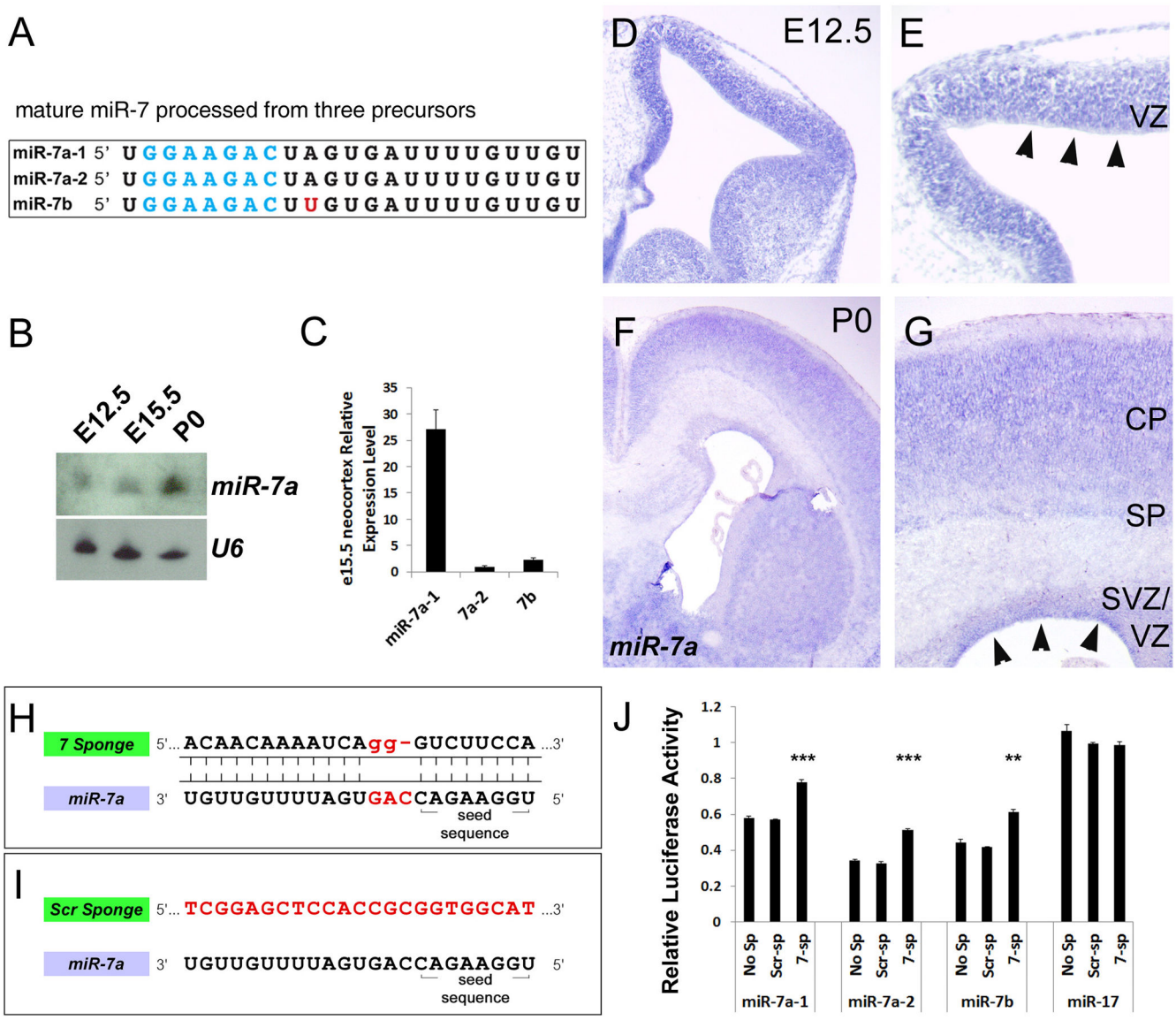

Figure 1. Endogenous miR-7 expression in mouse cortices and miR-7 sponge design

(A) Mature miR-7 sequences from each genomic locus.

(B) Northern blot detecting miR-7 expression using a locked nucleic acid (LNA) probe for *miR-7a* in E12.5, E15.5, and P0 cortices. U6 RNA was used as a loading control.

(C) Real time RT-PCR detecting miR-7 primary transcripts in the E15.5 cortex. Comparison is done to the miR-7a-2 expression level. $P = 0.000257$, n=3.

(D-G) miR-7 was expressed in neural progenitors in the ventricular zone (VZ) (arrowheads) and mature neurons throughout cortical development. Low (D,F) and high (E,G) power images of *in situ* hybridization using LNA probes for *miR-7a* in wild-type mouse cortices at E12.5 and P0. The subventricular zone (SVZ), subplate (SP) and cortical plate (CP) are labeled.

(H,I) Schematics representing the sponge sequences of one artificial, bulged binding site for miR-7 (H) or a scrambled (Scr) binding site (I).

(J) Relative activity of luciferase with a miR-7 binding site in its 3′UTR co-expressed with miR-7 or a control miRNA, and a sponge for miR-7 (7-sp), as in (H) or a scrambled sponge (Scr-sp), as in (I).

Data are presented as mean ± SEM; n≥3; *p* values in relation to No Sponge (No Sp) condition (**: $P < 0.01$, ***: $P < 0.001$). See also Figure S1.

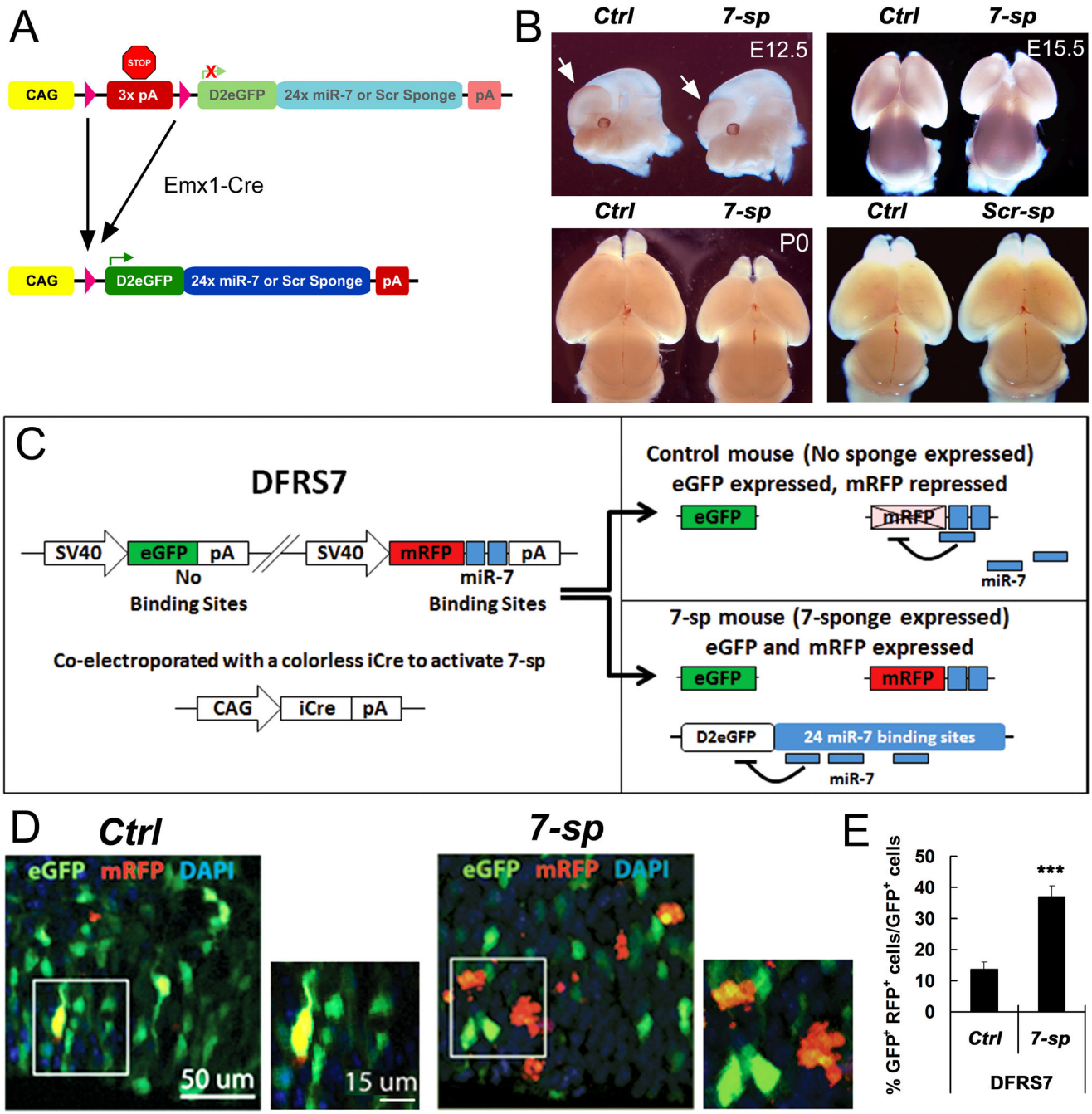

Figure 2. *miR-7 sponge* transgenic mice in which miR-7 function is blocked have smaller cortex

(A) The sponge transgene was driven by constitutively active *CAG* promoter followed by a floxed poly-A stop cassette, and D2*eGFP* gene containing 24 bulged binding sites for miR-7 or scrambled sites. Conditional activation by crossing with the cortical specific *Emx1-Cre* mouse line permitted expression of the miR-7 (*7-sp*) or scrambled (*Scr-sp*) sponge transcript only in the cortex.

(B) Cortical activation of miR-7 sponge resulted in significantly smaller cortex compared to littermate controls (*Ctrl*), with differences clearly visible by E12.5 (arrows), and significant

at E15.5 and P0. The cortex *of Scr-sp* mice had no differences compared to littermate controls.

(C) The sensor system to detect miR-7 function used two-color sensor plasmids in which eGFP was not sensitive to miRNA, while mRFP contained two binding sites for miR-7. This construct was co-electroporated with the *iCre* expression construct containing no fluorescent reporter into *7-sp* carrier embryos and wild type control (*Ctrl*) littermates.

(D) Co-electroporation of *iCre* with miR-7 sensor into *Ctrl* embryos revealed a small population of miR-7 negative cells in the dorsal cortex. Co-electroporation into *7-sp* carrier embryos revealed a significantly increased population of cells with blocked miR-7 activity.

(E) Quantification of the percentage of electroporated cells with blocked miR-7 activity as $eGFP^+mRFP^+$ cells/$eGFP^+$ cells.

Scale bars are labeled. Data are presented as mean ± SEM; n≥3 in all genotypes; *p* values in relation to control (***: $P < 0.001$). See also Figure S2.

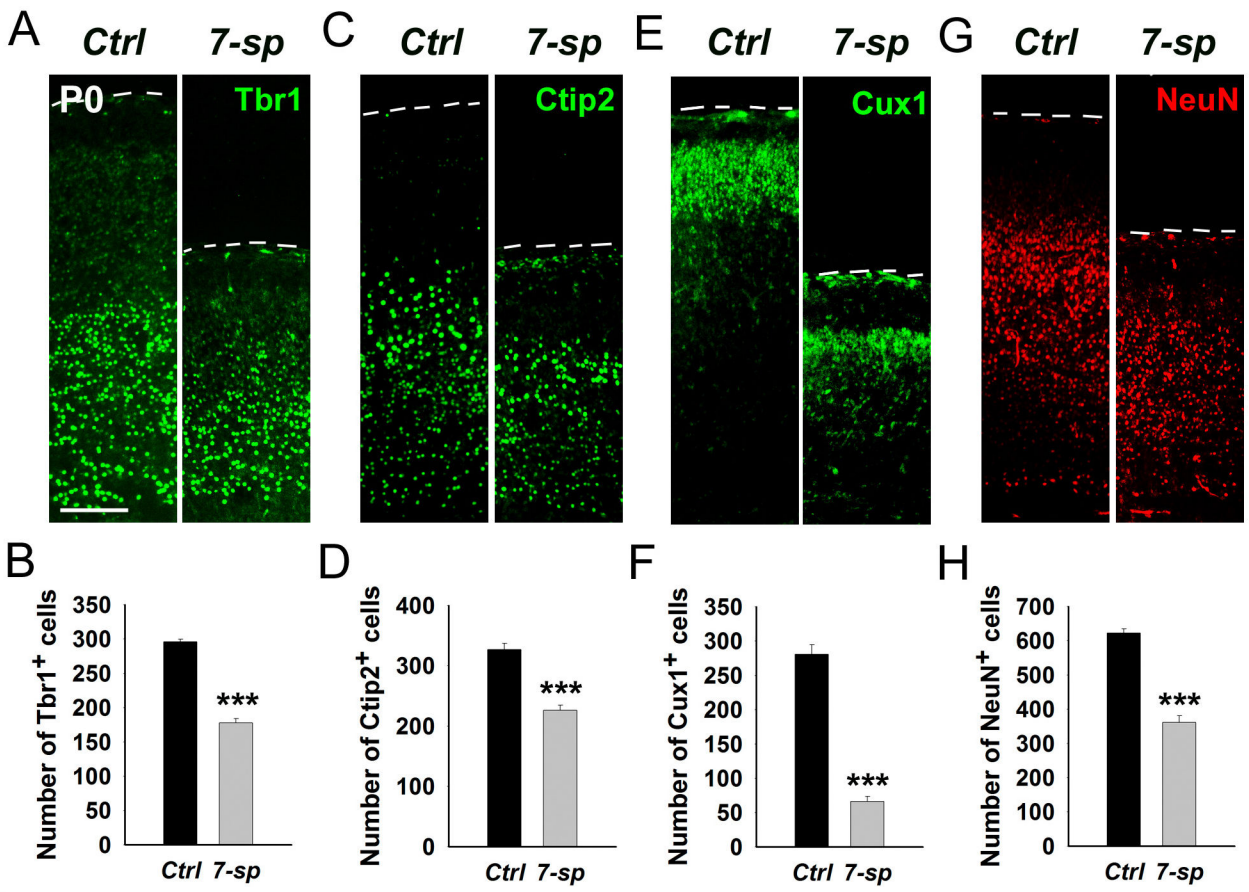

Figure 3. miR-7 sponge activation severely impairs neurogenesis of early- and late-born neurons

(A-D) miR-7 sponge (*7-sp*) activation caused a reduction in the number of early-born neurons labeled by Tbr1 or Ctip2, compared to controls (*Ctrl*).

(E,F) Late-born neurons labeled by Cux1 were also reduced in number.

(G,H) The overall number of NeuN-expressing neurons was reduced compared to controls. Scale bar = 100μM. Data are presented as mean ± SEM; n≥3 in all genotypes; *p* values in relation to control (***: $P < 0.001$). See also Figure S3.

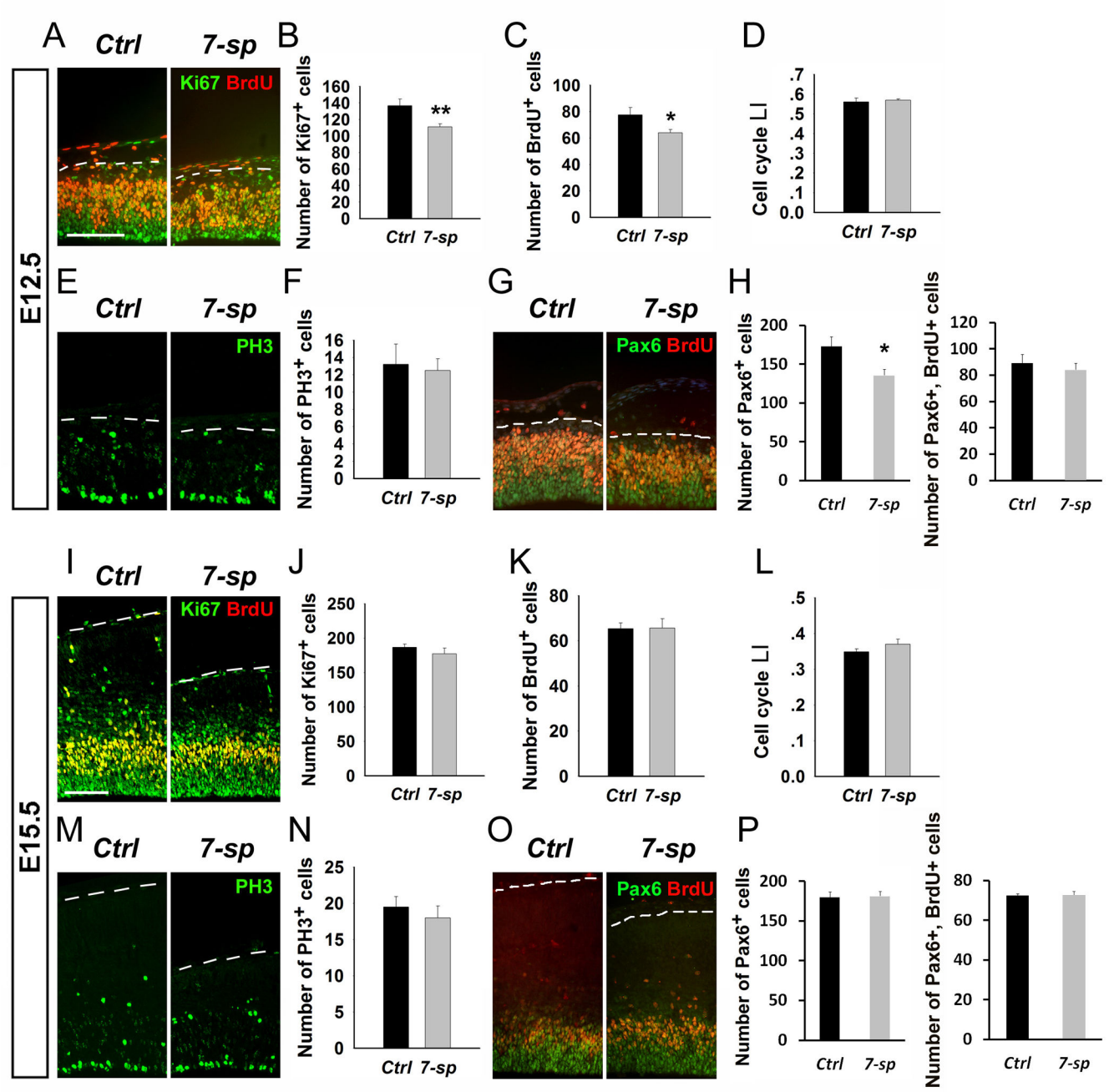

Figure 4. Radial glial cells (RGCs) are only mildly affected by loss of miR-7 activity during cortical development

(A-C) At E12.5, miR-7 sponge (*7-sp*) expression caused a slight reduction in the number of Ki67^{+} progenitors and a similarly small reduction in the number of cells incorporating BrdU in 30 minutes labeling, compared to controls (*Ctrl*).

(D) The cell cycle labeling index (LI) was unchanged from controls.

(E,F) The number of cells expressing PH3, a marker of cells in the M-phase of the cell cycle, was unchanged from controls.

(G,H) The number of RGCs expressing Pax6 was also slightly reduced. However, the number of RGCs incorporating BrdU was similar to controls.
(I-L) At E15.5, there were no longer differences in $Ki67^{+}$ cells or BrdU uptake, and the cell cycle LI remained equal to controls.
(M,N) The number of M-phase cells expressing PH3 was similar to controls.
(O,P) The number of RGCs expressing Pax6 was similar to controls, and the number of RGCs taking up BrdU was also similar to controls.
Scale bar = 50μM. Data are presented as mean ± SEM; n≥3 in all genotypes; *p* values in relation to control (*: $P < 0.05$; **: $P < 0.01$). See also Figure S4.

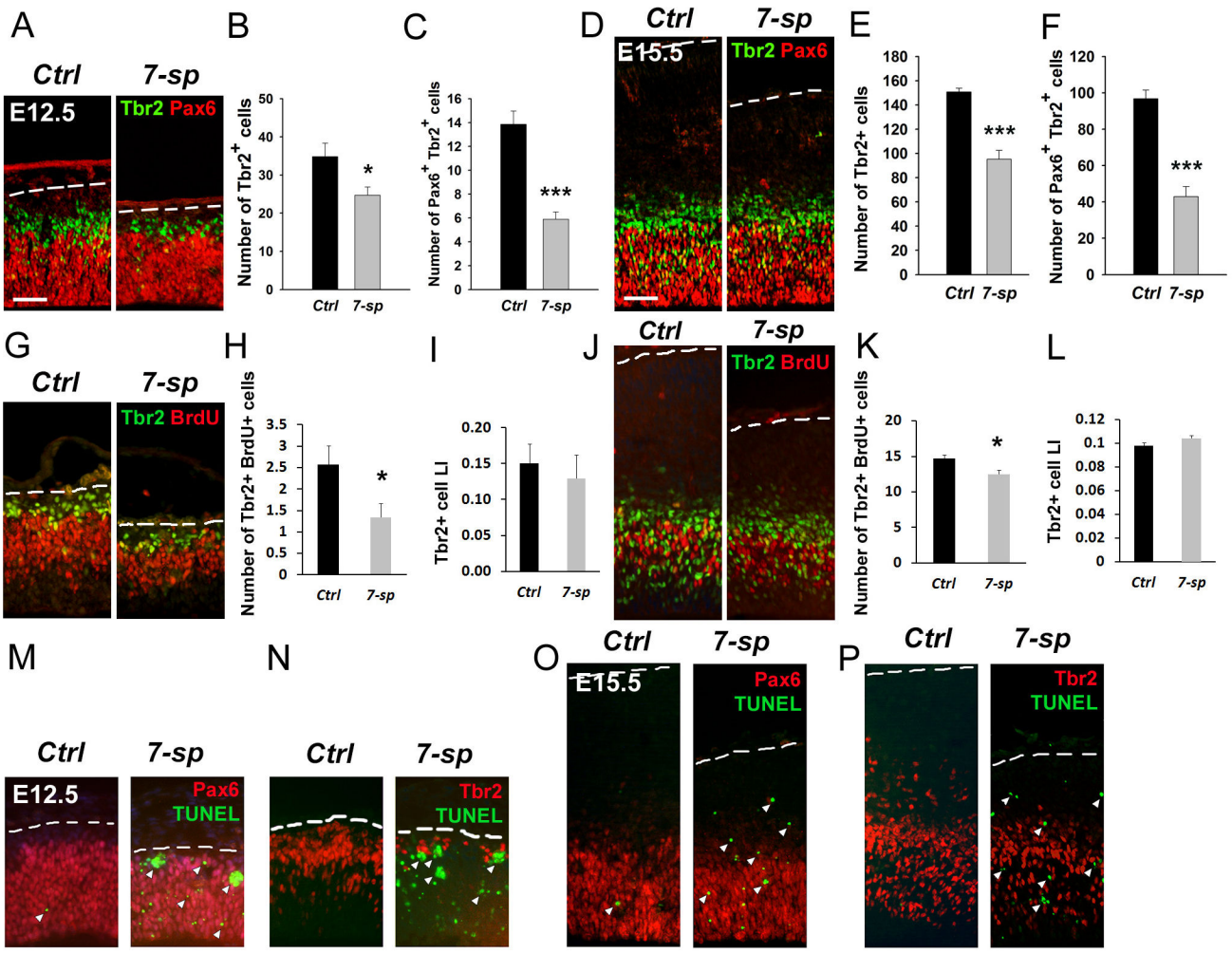

Figure 5. Reduced miR-7 activity results in impaired transition of intermediate progenitors and cell death

(A,B) At E12.5, loss of miR-7 function in *7-sp* cortices resulted in significantly fewer $Tbr2^+$ cells than in control cortices (*Ctrl*).

(C) The number of cells co-expressing Pax6 and Tbr2 was also dramatically reduced.

(D,E) At E15.5, the number of $Tbr2^+$ cells remained significantly reduced.

(F) The number of cells co-expressing Pax6 and Tbr2 also remained dramatically reduced at E15.5.

(G,H) At E12.5, the total number of $Tbr2^+$ cells was reduced, the number of $Tbr2^+$ cells incorporating BrdU was also lower than controls.

(I) The Tbr2 labeling index (LI) was similar to controls.

(J,K) At E15.5, the total number of $Tbr2^+$ cells was reduced, the number of $Tbr2^+$ cells incorporating BrdU was also lower than controls.

(L) The Tbr2 LI was similar to controls.

(M) Loss of miR-7 function caused significant cell death at E12.5. TUNEL staining (arrowheads) combined with Pax6 immunofluorescence.

(N) TUNEL staining combined with Tbr2 immunofluorescence revealed most TUNEL$^+$ cells in the subventricular zone (SVZ).
(O) Loss of miR-7 function caused significant cell death at E15.5. TUNEL staining combined with Pax6 immunofluorescence.
(P) TUNEL staining combined with Tbr2 immunofluorescence.
Scale bar = 50μM. Data are presented as mean ± SEM; n≥3 in all genotypes; *p* values in relation to control (*: $P < 0.05$; ***: $P < 0.001$). See also Figure S5.

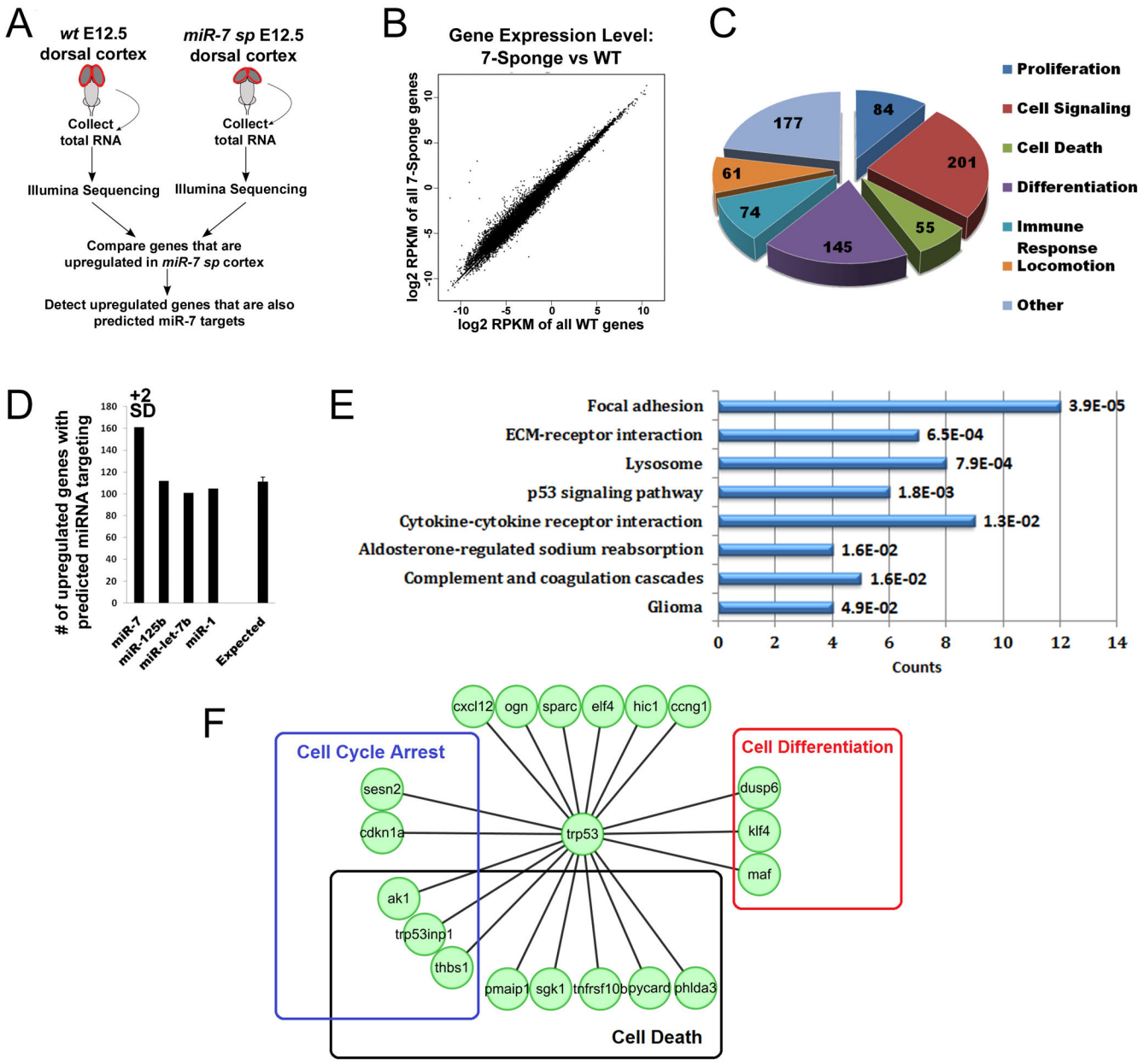

Figure 6. Cortical knockdown of miR-7 function causes upregulation of multiple targets, including many associated with the p53 signaling pathway

(A) Schematic outlining RNA isolation, sequencing, and analysis of RNA extracted from wild-type (*wt*) and miR-7 sponge (*sp*) cortices.

(B) Comparison of *7-sponge* RNA sequencing results with wild-type. Gene levels were expressed as $\log_2$RPKM. RPKM: the number of sequencing reads per kilobase of the transcript divided by one million.

(C) Gene ontology analysis using GOrilla on the 419 genes significantly upregulated in *7-sp* cortices.

(D) 162 upregulated genes were predicted targets of miR-7. Comparison of the 419 upregulated genes with target predictions for each of 35 neural miRNAs generated an

expected number of hits in a random neural sample. miR-7's 162 predicted and upregulated genes exceeded this by +2 standard deviations, while other miRNAs expressed in this tissue did not.

(E) The 162 upregulated miR-7 targets sorted by KEGG pathway analysis using DAVID revealed several pathways which are targeted by miR-7. The p53 signaling pathway that is known to govern progenitor checkpoint decisions and apoptosis was selected for further investigation.

(F) Manual literature search confirmation of genes in the p53 pathway uncovered 19 p53 pathway genes affected by loss of miR-7 function in E12.5 *7-sp* cortices.

Data are presented as mean ± SEM; n≥3 in all genotypes; *p* values in relation to control. See also Figure S6.

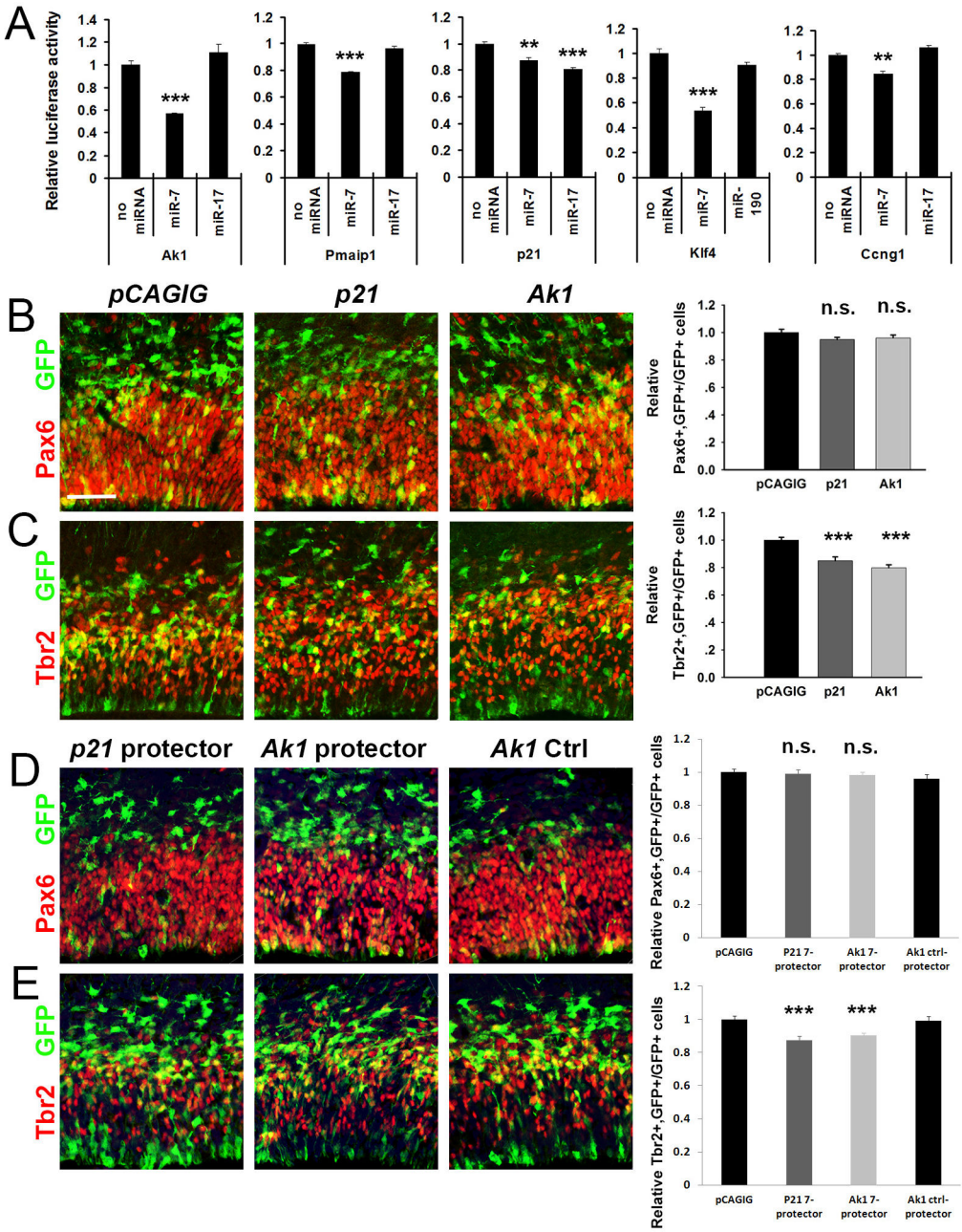

Figure 7. Genes in the p53 pathway are specific targets of miR-7 and are required for production of cortical intermediate progenitors

(A) Activity of *luciferase* containing the 3′UTRs of genes in the p53 pathway was reduced when co-expressed with miR-7. Control miRNA miR-17 did not affect *luciferase* activity except for with the *p21* 3′-UTR, since p21 is a known target of miR-17.

(B) Ectopic expression of *Ak1* or *p21* did not affect the number of Pax6^{+} cells compared to expression of the *pCAGIG* vector alone.

(C) Ectopic expression of *Ak1* or *p21* reduced the percentage of electroporated cells expressing Tbr2 compared to expression of the *pCAGIG* vector alone.

(D) Electroporation of *pCAGIG* along with an LNA target site protector oligos, designed to block miR-7's interaction with the *p21* 3′UTR (p21 protector), or the *Ak1* 3′UTR (Ak1 protector), did not affect the number of $Pax6^+$ cells compared to expression of the *pCAGIG* vector alone, or application of a target site protector designed to bind to the *Ak1* 3′UTR outside miR-7 binding sites (Ak1 Ctrl).

(E) Electroporation of *pCAGIG* together with the p21 protector, or Ak1 protector reduced the percentage of cells expressing Tbr2 compared to expression of the *pCAGIG* vector alone or Ak1 Ctrl.

Scale bar = 50μM. Data are presented as mean ± SEM; n≥3 in all constructs; *p* values in relation to control (**: $P < 0.01$; ***: $P < 0.001$; n.s.: none significant). See also Figure S6.